Atomistic pathways of the pressure-induced densification of quartz

Yunfeng Liang,[1,2,*] Caetano R. Miranda,[3] and Sandro Scandolo[4]

[1]*Environment and Resource System Engineering, Kyoto University, Kyoto 615-8540, Japan*

[2]*Key Laboratory of Materials Physics, Institute of Solid State Physics, Chinese Academy of Sciences, P.O. Box 1129, Hefei 230031, People's Republic of China*

[3]*Instituto de Física, Universidade de São Paulo, Caixa Postal 66318, São Paulo, SP 05315-970, Brazil*

[4]*The Abdus Salam International Centre for Theoretical Physics (ICTP), Trieste, Italy*

(Received 14 May 2015; published 2 October 2015)

When quartz is compressed at room temperature it retains its crystal structure at pressures well above its stability domain (0–2 GPa), and collapses into denser structures only when pressure reaches 20 GPa. Depending on the experimental conditions, pressure-induced densification can be accompanied by amorphization; by the formation of crystalline, metastable polymorphs; and can be preceded by the appearance of an intermediate phase, quartz II, with unknown structure. Based on molecular dynamic simulations, we show that this rich phenomenology can be rationalized through a unified theoretical framework of the atomistic pathways leading to densification. The model emphasizes the role played by the oxygen sublattice, which transforms from a bcc-like order in quartz into close-packed arrangements in the denser structures, through a ferroelastic instability of martensitic nature.

DOI: 10.1103/PhysRevB.92.134102 PACS number(s): 64.60.Bd, 81.05.Je, 81.05.Kf

Quartz was reported to collapse into a poorly crystallized metastable structure named quartz II at around 21 GPa [1], i.e., well into the region of stability of stishovite, followed either by amorphization [2–7] or by transition to metastable high-density crystalline polymorphs, e.g., $P2_1/c$ structure [8–10]. The pressure-induced amorphization (PIA) of quartz has been examined either from a thermodynamical point of view (as a density-driven transition to the reentrant highly viscous liquid [2,11], a phenomenology first observed in ice [12]), and from a mechanical standpoint (as an elastic/dynamic instability of the quartz lattice [13–20]), as well as from a crystallographic perspective, as the result of ordering and displacive mechanisms from a common parent structure [21]. Although each one of the above scenarios helps shed light on some specific aspects of the pressure-induced collapse, none of them accounts for established experimental observations such as the existence of quartz II [1,4,22], the post-quartz phase [8,9], and the microstructure of deformed quartz [1,4]. Three decades after the first report of PIA [1], a universal microscopic model of the pressure collapse is not yet available [23,24].

Atomistic simulations can in principle provide microscopic models [13–16,18,19,25–33], which can help rationalize the observed phenomenology. To date simulations with empirical potentials have confirmed the experimental evidence that nonhydrostatic pressure plays an important role [29], but simulations under nonhydrostatic conditions yield a crystalline structure with all silicon atoms in fivefold coordination with oxygen [29], which is not consistent with experiments. On the basis of first-principles simulations, where the interatomic potential is generated from a quantum mechanical solution of the electronic ground state, a structure with $P3_2$ ($Z = 9$) space group has been proposed for quartz II [30], as a result of an instability in the phonon spectrum of α-quartz at point $K(1/3,1/3,0)$. However, a different structure, with $C2$ space group, was obtained in another *ab initio* simulation under nonhydrostatic pressure [33] as well as in several classical calculations under hydrostatic pressure [31]. The comparison of calculated diffraction patterns for these model structures with the experimental patterns is not conclusive. On the other hand, Raman and IR measurements suggest only a minor structural change between quartz and quartz II [4,6,17]. No vibrational calculations have been reported so far for the quartz II theoretical candidates, however. Moreover, no evidence for an amorphous phase has emerged from previous *ab initio* calculations [30,33].

Inspired by the pioneering work of Sowa *et al.* [34], Binggeli *et al.* [28], and Dmitriev *et al.* [21] on the modifications of the oxygen packing upon compression of quartz, we employed a large cubic supercell consisting of 216 SiO_2 formula units constructed from $6 \times 6 \times 6$ cubic cells of the oxygen quasi-bcc sublattice that describes α-quartz at high pressure (Fig. 1). The supercell is commensurate with the phonon instability at point $K(1/3,1/3,0)$ and with all the three post–quartz crystalline phases reported so far ($C2$, $P3_2$ and $P2_1/c$). Such a choice makes it easy to control the orientation of the nonisotropic stress with respect to the oxygen sublattice [for example, the original c direction of quartz is parallel to the (111) direction of the supercell]. The relationship between the large cubic supercell and the primitive unit cell vectors of quartz is

$$\begin{pmatrix}\vec{A}\\ \vec{B}\\ \vec{C}\end{pmatrix} = \begin{pmatrix}6\vec{e}_x\\ 6\vec{e}_y\\ 6\vec{e}_z\end{pmatrix} = \begin{pmatrix}-4 & -2 & -2\\ 2 & 4 & -2\\ 2 & -2 & -2\end{pmatrix}\begin{pmatrix}\vec{a}\\ \vec{b}\\ \vec{c}\end{pmatrix},$$

where $\vec{A}$, $\vec{B}$, and $\vec{C}$ are the primitive vectors of the supercell; $\vec{e}_x$, $\vec{e}_y$, and $\vec{e}_z$ are the primitive vectors of the conventional cell of the underlying bcc sublattice; $\vec{a}$, $\vec{b}$, and $\vec{c}$ are the primitive vectors of α-quartz, i.e., $\vec{a} = (a/2, -\sqrt{3a/2}, 0)$, $\vec{b} = (a/2, \sqrt{3a/2}, 0)$, and $\vec{c} = (0, 0, c)$; and a and c are the α-quartz lattice parameters. It is important to remark that the

*Corresponding author. Mailing address: Kyoto University, Room C1-1-110, Kyotodaigaku-Katsura, Nishikyoku, Kyoto 615-8540, Japan. Tel: +81-75-383-3205. FAX: +81-75-383-3203. Liang.Yunfeng.5x@kyoto-u.ac.jp

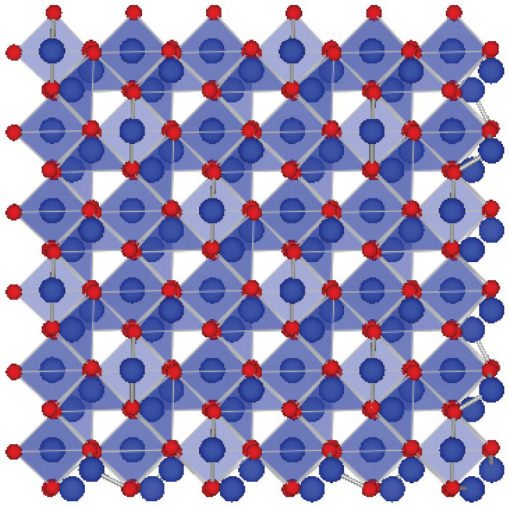

FIG. 1. (Color online) Simulation supercell containing 72 unit cells of α-quartz (648 atoms). Oxygen atoms are in red and Si atoms are in blue.

present work differs with respect to the study by Badro *et al.*, where a phase with fivefold Si coordination was found [29], in that the nonhydrostatic conditions are here imposed along different and well-defined directions relative to the oxygen sublattice. Following the strategy adopted for cristobalite [35] we apply small nonhydrostatic components to the stress tensor along the (001) direction of the bcc sublattice, which coincides with the (001) direction of the supercell. Structural optimizations at a given pressure or stress condition are performed starting with the α-quartz structure by allowing full relaxation of both lattice and internal coordinates.

The simulations were carried out using an interatomic force field optimized by best fit on first-principles (density functional theory) calculations [36]. The force field describes the structural and vibrational properties of most SiO_2 crystalline polymorphs, liquid, and glass [35–39] better than all the available force fields to which it has been compared so far. In particular, it describes the thermodynamic stability of the crystalline polymorphs of silica [35], at the same level of *ab initio* simulations, including the pressure dependence of the lattice constant and the phonon softening across the rutile-to-$CaCl_2$ transition [37,39].

We start by presenting the results of the structural optimization (0 K) under nonhydrostatic pressure conditions. We added a nonhydrostatic component of $\Delta\sigma_{zz} = 0.1P$ and $\Delta\sigma_{xx} = \Delta\sigma_{yy} = -0.05P$ (P is the average pressure of the system) to the stress tensor for tensile stress, and opposite signs for compressive stress. Under tensile stress we find that quartz transforms into a structure with $C2$ space group when pressure reaches 22 GPa (i.e., $\sigma_{zz} = 19.8$ GPa, $\sigma_{xx} = \sigma_{yy} = 23.1$ GPa). The $C2$ structure is characterized by an fcc oxygen sublattice [40] and the transformation of the oxygen sublattice from bcc to fcc clearly follows the Bain path, as expected for tensile stress along the [100] bcc direction. Under compressive stress quartz transforms into a monoclinic structure of space group $P2_1$ ($Z = 6$) with an hcp oxygen sublattice, along the Burgers path, when pressure reaches 36 GPa (i.e., $\sigma_{zz} = 39.6$ GPa, $\sigma_{xx} = \sigma_{yy} = 34.2$ GPa). In the $P2_1$ structure one-third of the silicon atoms are in fourfold coordination and two-thirds are in sixfold coordination. Compressing the $P2_1$ structure further, we obtained at 150 GPa the $P2_1/c$ structure, first proposed for SiO_2 in Ref. [27] and recently observed in Ref. [8]. The $P2_1/c$ structure has an hcp oxygen sublattice with silicon in octahedral coordination, and can be recovered, in our simulations, to 0 GPa. The relaxed cell parameters at 0 GPa are $a = 6.76$, $b = 4.14$, $c = 5.02$ Å, $\beta = 101.0$, which are in excellent agreement with experimental data $a = 6.92$, $b = 4.10$, $c = 5.03$ Å, $\beta = 102.0$ [8].

Based on the results of the non-hydrostatic calculations it is clear that non-hydrostaticity is effective in controlling the transformation of the oxygen sublattice from bcc to fcc or hcp, depending on the sign of the non-hydrostatic component, similarly to what observed in cristobalite [35].

We now turn to the results of the structural optimization under hydrostatic conditions. Under hydrostatic conditions we obtain quartz below 38 GPa, and two structures with the same space group ($P3_2$), but with different silicon coordinations between 38 and 46 GPa and above 46 GPa, respectively. This is consistent with what Wentzcovitch *et al.* [30] found with *ab initio* methods at 33 GPa and 40 GPa, respectively. We named the two high-pressure structures $P3_2$ and hp-$P3_2$ (high-pressure-$P3_2$) structure, respectively. The structural parameters, as well as the coordination, of the two structures are in excellent agreement with first-principles calculations. The oxygen sublattice in $P3_2$ structure is still bcc-like. This is consistent with the results of the nonhydrostatic calculations: while small compressive or tensile components readily activate Bain and Burgers path transformations, respectively, hydrostaticity leads to a frustrated situation in which the outcome may be sensitive to local fluctuations or to concomitant instabilities, as already observed in Ref. [20]. In the specific case of $P3_2$, this structure is known to result from a dynamical instability of the quartz phase at a finite wave vector [30].

In order to check the effects of local fluctuations in the hydrostatic case, we carried out a series of molecular dynamics (MD) hydrostatic simulations at finite temperature (300–1000 K), starting from quartz as well as from the $P3_2$ structure. Heating up the $P3_2$ structure to room temperature (300 K) yields, above 38 GPa (and at all pressures if $T = 1000$ K) an amorphous structure (we define a structure amorphous if the space group analysis yields no symmetry with a tolerance of ~0.1 Å). Room-temperature hydrostatic MD simulations of quartz yield amorphous structures similar to the one obtained upon heating the $P3_2$ structure, although the transformation pressures and paths appear to depend on the compression rate. At low rate (2 GPa increments every 21.7 ps, namely 30 000 steps) the amorphous structure is obtained from quartz through an intermediate $P3_2$ structure at 32–38 GPa, while at high rate (4 GPa increments every 21.7 ps) the amorphous structure is obtained directly from quartz at 32 GPa.

A coordination analysis shows the amorphous structure obtained in the above simulations is a mixture of fourfold and sixfold coordinated silicon with minimal fivefold silicon. The pair analysis [35,40] shows that the amorphous structure is a mixture of fcc and hcp oxygen sublattice (the ratio varies from pressure to pressure). As shown in Figs. 2(a)–2(c), the amorphous structure at 40 GPa is evidently disordered if viewed along the $x-y$ and $y-z$ plane, but presents a quite

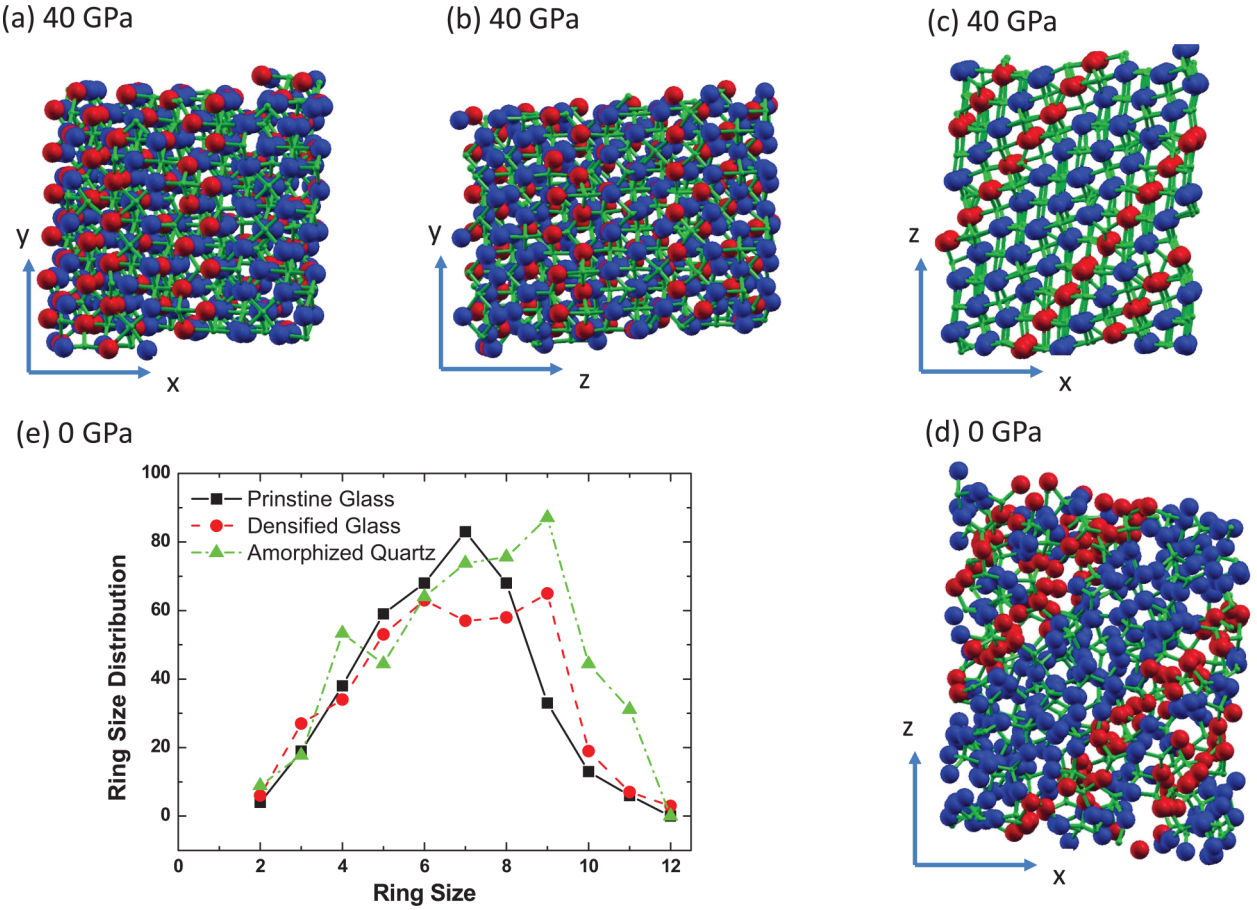

FIG. 2. (Color online) (a–c) Snapshot of the amorphous structure obtained from compressed quartz at 40 GPa and 300 K, viewed along the three Cartesian axes. The red and blue spheres are oxygen atoms in fcc and hcp local arrangement as determined based on the HA index [35,40]. (d) Same view as (c) after pressure release to ambient pressure. (e) Ring-size distribution for three different amorphous samples.

ordered structure in the $x-z$ plane. We then decompressed the sample at room temperature by MD simulations, with stepwise decrements of 5 GPa every 21.7 ps. We obtained a densified glass, which totally loses the pseudocrystalline order in the $x-z$ plane and the oxygen ordering [shown in Fig. 2(d)], which is no longer close packed. The density of the recovered sample is 2.7 g/cm^3 and the Si coordination is approximately 4. The ring statistics analysis [Fig. 2(e)] shows that the topology is similar to that found in densified glass quenched from high pressure [38]. We conclude that the densified glass obtained in our simulations is a good model for the material recovered in experiments [2,3,5].

The hydrostatic simulations confirm that local fluctuations can induce the formation of a disordered structure and the structural similarity between the amorphous structure obtained from simulations and the pressure-induced amorphous structure obtained experimentally suggests that PIA is the result of the collapse of the oxygen bcc sublattice into microscopically inhomogeneous close-packed arrangements induced by locally inhomogeneous stress fields in the sample, as suggested by Toledano and Machon [20]. We remark that the proposed mechanism differs from the mechanism described in [21], which was instead based on a reconstructive disordering of the cation sites in an otherwise quasi-bcc oxygen sublattice. Disordering in our model is caused by the inhomogeneity of the oxygen sublattice domains and does not require a reconstructive process.

Based on the above results we now extend the discussion to the origin and nature of quartz II. It is instructive to summarize the main evidences that have been brought in support of an intermediate phase between quartz and amorphization or formation of denser, octahedral phases of silica. From x-ray diffraction the formation of quartz II has been associated [1] with the convergence of the (110) and (102) peaks, as shown in Fig. 3(a). Notice that the lines around 3.7 and 2.7 Å originally proposed to correspond to quartz II have been shown to originate from a different post–quartz crystalline phase by Kingma *et al.* [9]. Raman spectroscopy shows that quartz II has essentially the same spectrum as quartz, with the exception of a sizable decrease of the intensity of some peaks, and the appearance of a weak new peak at 675 cm^{-1} [41]. Finally, the appearance of quartz II has been associated with the formation of crystalline or amorphous lamellae whose boundaries were found to be primarily oriented parallel to the {102} crystallographic plane of the original quartz crystal [1,4]. This twinned state of quartzlike structures [1] has been reported to account for the elastically anisotropic behavior of the recovered sample [7].

Here we show that the above evidences do not require the existence of an intermediate phase. The convergence of the

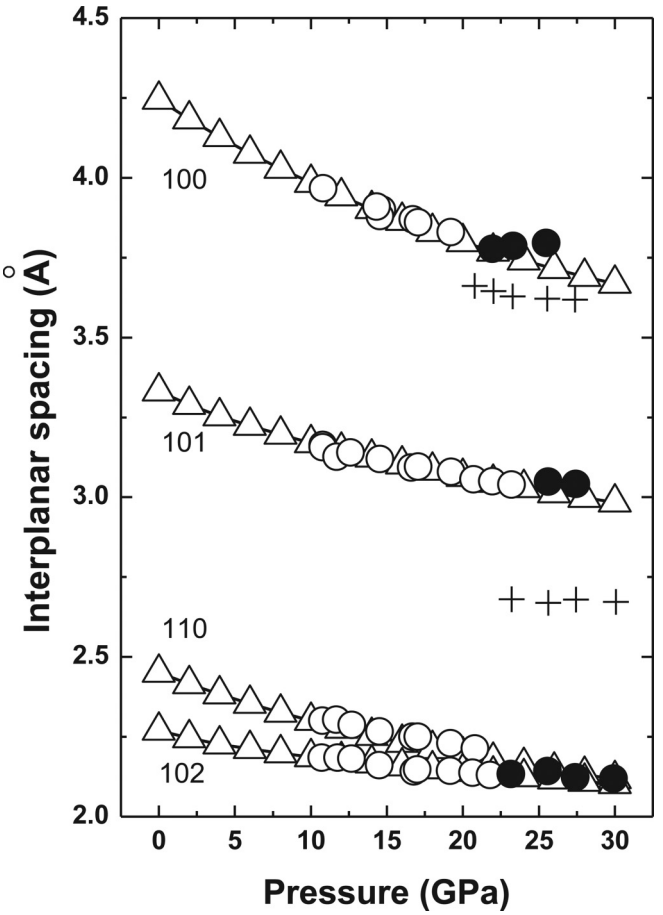

FIG. 3. Calculated interplanar distance as a function of pressure for quartz (open triangles), compared with experiments [1] for quartz (open circles), quartz II (solid circles), and a high-pressure structure (crosses).

diffraction spacings agrees with the calculated spacings for quartz under compression, which is a consequence of the bcc symmetrization of quartz. The Raman spectrum calculated with density functional theory [42] of quartz at 22 GPa agrees well with experiments, including relative intensities (Fig. 4). The peak at 675 cm^{-1} is not present in the calculated spectrum of quartz, but we notice that that a peak at similar frequencies exists in the spectrum calculated for the $C2$ structure which is obtained, in our simulations, precisely at 22 GPa, in the presence of nonhydrostatic pressure. On the other hand it is clear from Fig. 4 that the $C2$ and $P3_2$ structures must be ruled out as candidates for quartz II. Finally, we notice that the {102} crystallographic plane of quartz indeed coincides with the {100} plane of the oxygen bcc sublattice. Lamellae parallel to the bcc {100} plane are routinely seen as a precursor in the bcc-fcc martensitic transformations in metals [43]. We therefore argue that the appearance of lamellae at 22 GPa is due to local nonhydrostatic pressure fields which cause the collapse of quartz into structures with local $C2$ (or other close-packed) structures [20]. In agreement with past reports, the $C2$ structure reverts back to quartz if decompressed to 5 GPa [31]. This is consistent with the experimentally reported reversibility of the transition [1].

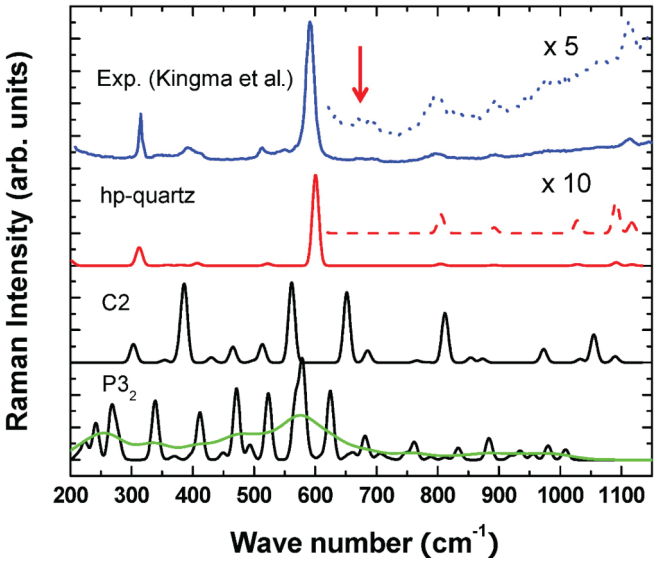

FIG. 4. (Color online) Calculated Raman spectra of hp-quartz, $C2$ and $P3_2$ at 24 ± 2 GPa, compared with experiments for quartz II at 24.5 GPa [4]. Theoretical frequencies are rescaled by +5% as in Ref. [42] and the spectra are convoluted with a uniform Gaussian broadening having 4.0 cm^{-1} width.

In summary, we have presented a comprehensive atomistic picture of the pressure-induced densification of quartz, where a crucial role is played by the collapse of the oxygen sublattice into a close-packed arrangement. Our analysis explains the influence of nonhydrostatic pressure conditions on the densification and provides a unified framework that rationalizes the observation of crystalline as well as amorphous structures. In particular, we show that quartz II is not a distinct phase, but rather a manifestation of the precursors of the shear instability which drives the bcc oxygen sublattice into close-packed structures. Similar conclusions were reached analyzing the oxygen sublattice in cristobalite, suggesting that the mechanisms described here could be more general and relevant in the understanding of the densification of other tetrahedral silicates, among them coesite, whose pressure-induced collapse has been recently shown to result in the formation of several low-symmetry metastable structures [44].

ACKNOWLEDGMENTS

We would like to thank Nadia Binggeli for the critical assistance with constructing the cubic bcc cell used in this study, Russell J. Hemley for discussions of quartz II, and appreciate the invaluable help from Wei Liu, Changsong Liu, Javier A. Montoya. and Riccardo Mazzarello. The research was financially supported by the National Natural Science Foundation of China (No. 11274306). C.R.M. acknowledges the financial support provided by the Brazilian agencies CAPES, CNPq, and Fapesp and the Japan Society for the Promotion of Science (JSPS).

[1] K. J. Kingma, R. J. Hemley, H.-K. Mao, and D. R. Veblen, New High-Pressure Transformation in α-Quartz, Phys. Rev. Lett. **70**, 3927 (1993).

[2] R. J. Hemley, A. P. Jephcoat, H.-K. Mao, L. C. Ming, and M. H. Manghnani, Pressure-induced amorphization of crystalline silica, Nature **334**, 52 (1988).

[3] R. R. Winters, A. Garg, and W. S. Hammack, High-Resolution Transmission Electron Microscopy of Pressure-Amorphized α-Quartz, Phys. Rev. Lett. **69**, 3751 (1992).

[4] K. J. Kingma, C. Meade, R. J. Hemley, H.-K. Mao, and D. R. Veblen, Microstructural observations of α-quartz amorphization, Science **259**, 666 (1993).

[5] R. J. Hemley, Pressure dependence of Raman spectra of SiO_2 polymorphs: α-quartz, coesite and stishovite, in *High-Pressure Research in Mineral Physics*, edited by M. H. Manghnani and Y. Syono (Terra Scientific, Tokyo and American Geophysical Union, Washington, DC, 1987), p. 347.

[6] Q. Williams, R. J. Hemley, M. B. Bruger, and R. Jeanloz, High-pressure infrared spectra of α-quartz, coesite, stishovite and silica glass, J. Geophys. Res. **98**, 22157 (1993).

[7] L. E. McNeil and M. Grimsditch, Pressure-Amorphized SiO_2 α-Quartz: An Anisotropic Amorphous Solid, Phys. Rev. Lett. **68**, 83 (1992).

[8] J. Haines, J. M. Leger, F. A. Gorelli, and M. Hanfland, Crystalline Post-Quartz Phase in Silica at High Pressure, Phys. Rev. Lett. **87**, 155503 (2001).

[9] K. J. Kingma, H.-K. Mao, and R. J. Hemley, Synchrotron x-ray diffraction of SiO_2 to multimegabar pressures, High Press. Res. **14**, 363 (1996).

[10] Y. Tsuchida and T. Yagi, New pressure-induced transformations of silica at room temperature, Nature **347**, 267 (1990).

[11] J. Badro, J. L. Barrat, and P. Gillet, Melting and pressure-induced amorphization of quartz, Europhys. Lett. **42**, 643 (1998).

[12] O. Mishima, L. D. Calvert, and E. Whalley, Relationship between melting and amorphization of ice, Nature **310**, 393 (1984).

[13] J. S. Tse and D. D. Klug, Mechanical Instability of α-Quartz: A Molecular Dynamics Study, Phys. Rev. Lett. **67**, 3559 (1991).

[14] N. Binggeli and J. R. Chelikowsky, Elastic Instability in α-Quartz Under Pressure, Phys. Rev. Lett. **69**, 2220 (1992).

[15] S. L. Chaplot and S. K. Sikka, Molecular-dynamics simulation of pressure-induced crystalline-to-amorphous transition in some corner-linked polyhedral compounds, Phys. Rev. B **47**, 5710 (1993).

[16] G. W. Watson and S. C. Parker, Dynamical instabilities in α-quartz and α-berlinite: A mechanism for amorphization, Phys. Rev. B **52**, 13306 (1995).

[17] P. Richet and P. Gillet, Pressure-induced amorphization of minerals: a review, Eur. J. Mineral. **9**, 907 (1997).

[18] M. S. Somayazulu, S. M. Sharma, and S. K. Sikka, Structure of a New High Pressure Phase in α-Quartz Determined by Molecular Dynamics Studies, Phys. Rev. Lett. **73**, 98 (1994).

[19] N. Binggeli, J. R. Chelikowsky, and R. M. Wentzcovitch, Simulating the amorphization of α-quartz under pressure, Phys. Rev. B **49**, 9336 (1994).

[20] P. Toledano and D. Machon, Structural mechanism leading to a ferroelastic glass state: Interpretation of amorphization under pressure, Phys. Rev. B **71**, 024210 (2005).

[21] V. P. Dmitriev, P. Toledano, V. I. Torgashev, and E. K. H. Salje, Theory of reconstructive phase transitions between SiO_2 polymorphs, Phys. Rev. B **58**, 11911 (1998).

[22] E. Gregoryanz, R. J. Hemley, H.-K. Mao, and P. Gillet, High-Pressure Elasticity of α-Quartz: Instability and Ferroelastic Transition, Phys. Rev. Lett. **84**, 3117 (2000); High-Pressure Elasticity of α-Quartz: Instability and Ferroelastic Transition, *ibid.* **90**, 079702 (2003).

[23] D. Machon, F. Meersman, M. C. Wilding, M. Wilson, and P. F. McMillan, Pressure-induced amorphization and polymorphism: Inorganic and biochemical systems, Prog. Mater. Sci. **61**, 216 (2014).

[24] A. R. Oganov, Thermodynamics, phase transitions, equations of state, and elasticity of minerals at high pressures and temperatures, in *Treatise of Geophysics*, 2nd ed. (Elsevier, Amsterdam, 2015), pp. 179–202.

[25] L. P. Huang, M. Durandurdu, and J. Kieffer, Transformation pathways of silica under high pressure, Nat. Mater. **5**, 977 (2006).

[26] R. Martonak, D. Donadio, A. R. Oganov, and M. Parrinello, Crystal structure transformations in SiO_2 from classical and ab initio metadynamics, Nat. Mater. **5**, 623 (2006).

[27] D. M. Teter, R. J. Hemley, G. Kresse, and J. Hafner, High Pressure Polymorphism in Silica, Phys. Rev. Lett. **80**, 2145 (1998).

[28] N. Binggeli and J. R. Chelikowsky, Structural transformation of quartz at high pressures, Nature **353**, 344 (1991).

[29] J. Badro, J. L. Barrat, and P. Gillet, Numerical Simulation of α-Quartz under Nonhydrostatic Compression: Memory Glass and Five-Coordinated Crystalline Phases, Phys. Rev. Lett. **76**, 772 (1996).

[30] R. M. Wentzcovitch, C. da Silva, J. R. Chelikowsky, and N. Binggeli, A New Phase and Pressure Induced Amorphization in Silica, Phys. Rev. Lett. **80**, 2149 (1998).

[31] C. Campana, M. H. Muser, J. S. Tse, D. Herzbach, and P. Schoffel, Irreversibility of the pressure-induced phase transitions of quartz and the relation between three hypothetical post-quartz phases, Phys. Rev. B **70**, 224101 (2004).

[32] J. S. Tse, D. D. Klug, Y. Le Page, and M. Bernasconi, High-pressure four-coordinated structure of SiO_2, Phys. Rev. B **56**, 10878 (1997).

[33] N. Choudhury and S. L. Chaplot, *Ab initio* studies of phonon softening and high-pressure phase transitions of α-quartz SiO_2, Phys. Rev. B **73**, 094304 (2006).

[34] H. Sowa, Changes of oxygen packing of low quartz and ReO_3-structure under pressure, Z. Kristallogr. **184**, 257 (1988).

[35] Y. Liang, C. R. Miranda, and S. Scandolo, Tuning Oxygen Packing in Silica by Non-Hydrostatic Pressure, Phys. Rev. Lett. **99**, 215504 (2007).

[36] P. Tangney and S. Scandolo, An ab initio parameterised interatomic force field for silica, J. Chem. Phys. **117**, 8898 (2002).

[37] Y. Liang, C. R. Miranda, and S. Scandolo, Infrared and Raman spectra of silica polymorphs from an ab initio parametrized polarizable force field, J. Chem. Phys. **125**, 194524 (2006).

[38] Y. Liang, C. R. Miranda, and S. Scandolo, Mechanical strength and coordination defects in compressed silica glass: molecular dynamics simulations, Phys. Rev. B **75**, 024205 (2007).

[39] D. Herzbach, K. Binder, and M. H. Muser, Comparison of model potentials for molecular dynamics simulations of silica, J. Chem. Phys. **123**, 124711 (2005).

[40] The local strucure was analyzed based on the polyhedra distributions determined with the so-called HA index (pair analysis technique): J. D. Honeycutt and H. C. Andersen, Molecular dynamics study of melting and freezing of small Lennard-Jones clusters, J. Phys. Chem. **91**, 4950 (1987).

[41] K. J. Kingma, Pressure-induced transformation in SiO_2, Ph.D. thesis, Johns Hopkins University, 1994.

[42] M. Lazzeri and F. Mauri, First-principles calculation of vibrational Raman spectra in large systems: Signature of small rings in crystalline SiO_2, Phys. Rev. Lett. **90**, 036401 (2003).

[43] Z. Nishiyama, *Martensitic Transformation*, (Academic Press, New York, San Francisco, and London, 1978).

[44] Q. Y. Hu, J.-F. Shu, A. Cadien, Y. Meng, W. G. Yang, H. W. Sheng, and H. -K. Mao, Polymorphic phase transition mechanism of compressed coesite, Nat. Commun. **6**, 6630 (2015).